NJC

Accepted Manuscript

This is an *Accepted Manuscript*, which has been through the Royal Society of Chemistry peer review process and has been accepted for publication.

Accepted Manuscripts are published online shortly after acceptance, before technical editing, formatting and proof reading. Using this free service, authors can make their results available to the community, in citable form, before we publish the edited article. We will replace this *Accepted Manuscript* with the edited and formatted *Advance Article* as soon as it is available.

You can find more information about *Accepted Manuscripts* in the Information for Authors.

Please note that technical editing may introduce minor changes to the text and/or graphics, which may alter content. The journal's standard Terms & Conditions and the Ethical guidelines still apply. In no event shall the Royal Society of Chemistry be held responsible for any errors or omissions in this *Accepted Manuscript* or any consequences arising from the use of any information it contains.

ROYAL SOCIETY OF CHEMISTRY

www.rsc.org/njc

New Journal of Chemistry

RSCPublishing

ARTICLE

Controlled Solvothermal Synthesis of CuS Hierarchical Structures and Their Natural-Light-Induced Photocatalytic Properties

Cite this: DOI: 10.1039/xoxxoooooox

Received ooth January 2012,
Accepted ooth January 2012

DOI: 10.1039/xoxxoooooox

www.rsc.org/

Zahra Hosseinpour[a,b*], Abdolali Alemi[a], Ali Akbar Khandar[a], Xiujian Zhao[c], Yi Xie[b,c*]

Abstract

Hierarchical structures of covellite CuS are successfully prepared by a facile one-step solvothermal approach using $CuCl_2 \cdot 2H_2O$ and sodium thiosulfate as the copper and sulfur precursors, respectively. The as-synthesized self-assembly hierarchical structures are characterized by using powder X-ray diffraction (XRD), field emission-scanning electron microscopy (FESEM), high-resolution transmission electron microscopy (HRTEM), UV-vis-NIR spectroscopy and photoluminescence (PL) spectra. The experimental XRD patterns and HRTEM confirm the formation of hexagonal structure of covellite CuS. The solvent volume ratios of ethylene glycol (EG) to ethanol (ET) are revealed to play a critical role in the morphology control of the hierarchical structures. The photocatalytic activity of the resulting CuS photocatalysts is investigated by the degradation of the organic methylene blue (MB) under natural light irradiation, which suggests much higher photoactivity of the CuS hierarchical structures than that of commercial CuS and TiO_2 photocatalyst.

1. Introduction

Semiconductor photocatalysis technology has attracted much attention since Fujishima and Honda reported the water splitting on TiO_2 under UV irradiation in 1972.[1] This technology with TiO_2 is the most widely studied in the past years due to its nontoxicity, chemical stability and cost effectiveness. It has demonstrated promising chemical conversion of solar energy and thus has been utilized in various fields such as hydrogen generation,[2] removal of organic pollutants and bacteria from water or air.[3-5] However, the practical application of TiO_2 is restricted due to its wide band gap which limits the utilization of ultraviolet energy from sunlight. To solve this problem, various techniques to extend the use of visible energy and thus to improve the conversion efficiency were widely explored, such as doping and decoration of TiO_2 with metal, nonmetal and semiconductors with narrow band gaps.[6-9] Besides these efforts, other photocatalysts such as sulfides, nitrides, chlorides, Bi-based oxides, etc., which can effectively utilize visible light, have been also widely researched in recent years.[10-17]

In particular, copper sulphides are of great interest due to their extraordinary optical and electrical properties which can bring many potential applications. The stoichiometry of copper sulfide varies from CuS_2 at the copper-deficient side to Cu_2S at the copper-rich side. The covellite CuS is one of the most intensively studied copper sulfides due to its unique physical and chemical properties and its great potential applications in many fields such as photocatalysis,[18] low-temperature superconductors,[19, 20] optical filters and surperionic materials,[21] nanometer-scale switches,[22] lithium-ion batteries,[23] chemical sensors,[24] and thermoelectric cooling material.[25] The studies on photocatalysis of covellite CuS focus mainly on visible light source thanks to its narrow band gap and good optical absorption properties in the visible-NIR region.[10]

On the other side, the physico-chemical properties, performances and functionalities are observed to be significantly dependent on the morphologies, nanostructure, composition and crystallinity of materials.[26-28] With respect to morphological control, many efforts including hot injection,[29] heat up,[30, 31] single source precursor,[32] and solvothermal [33, 34] have been devoted to fabricating covellite CuS of disks,[29, 30] wires,[32] spheres,[33, 35] sheets,[36] and flowers.[37] In particular, hierarchical CuS nanostructures have demonstrated promising application in photocatalysis of degradation for organic dyes.[38, 39] The hierarchical structures can significantly enhance the performance of materials due to their nanosized building blocks and micro- or submicro-sized assemblies.[16, 40] Hence, investigation of the controlled hierarchical semiconductor nanostructures is of paramount industrial and scientific importance.

Among the above-mentioned synthesis approaches, solvothermal method, a low-cost, low-risk and easy-to-operate synthetic technique, has been reported to be effective for fabricating various hierarchical structures.[39] In the present work, we propose a facile and reproducible solvothermal procedure to synthesize hierarchical CuS with controllable shape and size by tuning the reaction solvents and their volume ratios. The natural-light-induced photocatalytic activity for the degradation of dye methylene blue (MB) is investigated, from which the effect of solvents is discussed and the photoactivity of the

as-synthesized CuS samples is compared with that of commercial CuS and TiO_2 photocatalysts.

2. Experimental

2.1. Chemicals

Copper (II) chloride ($CuCl_2 \cdot 2H_2O$ 99%), sodium thiosulfate ($Na_2S_2O_3$, 99.5%), ethylene glycol ($C_2H_6O_2$ (EG), >99%), ethanol (ET, anhydrous, 99.9%), and N, N, dimethylformamide (DMF, >99.5%) were purchased from Merck Company. All chemicals were used as received without further purification.

2.2. Synthesis of CuS hierarchical structures

In a typical synthesis, 1 mmol $CuCl_2 \cdot 2H_2O$ was dissolved in a 15 mL mixture solution consisting EG and ET (with a variable volume ratios of EG:ET from 1:0 to 1:3) and stirred for 30 min. Then sodium thiosulfate ($Na_2S_2O_3$) solution prepared by dissolving 1.1 mmol of $Na_2S_2O_3$ in 15 mL mixture solution of EG and ET was added into the Cu solution under magnetic stirring. The mixture solution was then transferred into a Teflon-lined autoclave, sealed, and maintained at 150 ^oC for 24 h. The resulting CuS sample was cooled to room temperature, followed by cleaning several times with distilled water and ethanol, and drying in vacuum at 60 ^oC for 4 h. In a comparison synthesis procedure, CuS hierarchical structures were also prepared by using only DMF instead as solvent however preserving all other above-mentioned reaction parameters.

2. 3. Characterization

The crystallographic information of the samples was obtained using powder X-ray diffraction (XRD) and high-resolution transmission electron microscopy (HRTEM). The XRD patterns were recorded by Siemens D5000 using Cu Kα radiation (λ =1.5406˚A) in a scanning 2θ range of 10-70˚. The HRTEM images were obtained with JEOL JEM-2010F microscopes operating at 200 kV. Additionally, the morphology of the as-obtained CuS samples was examined with a LEO-1430VP scanning electron microscope operating at 15 kV. Extinction spectra of the resulting materials dispersed in tetrachloroethylene (TCE) were measured in 1 cm path length quartz cuvettes using a Varian Cary 5000 UV-vis-NIR spectrophotometer. The photoluminescence (PL) spectra were recorded on a Varian Cary Eclipse fluorescence spectrophotometer with an intense Xenon flash lamp with excitation wavelength of 370 nm. Adsorption-desorption isotherms of N_2 were measured by an automatic adsorption system (Belsorp mini II, BEL Japan Inc.) at 77 K (liquid nitrogen temperature). Prior to the measurement, the samples were pre-treated at 373 K in a vacuum for 15 h. The surface area and pore size were determined by applying the conventional Brunauer-Emmett-Teller (BET) method and Barrett-Joyner-Halenda (BJH) equation, respectively.

2. 4. Measurement of photocatalytic activity

The photocatalytic activity of synthesized CuS samples in degradation of methylene blue (MB) was investigated in the presence of H_2O_2 (30%, w/w) under natural light. Typically, 0.01 g of CuS photocatalyt was added in 40 mL of MB aqueous solution (2×10^{-5} M) and sonicated for 10 min in a dark room to establish an adsorption/desorption equilibrium between MB molecules and the surface of the photocatalyst. Afterwards, 0.1 mL of H_2O_2 was added into the mixture solution, followed by further magnetically stirring under natural light. All these experiments are performed at the same time in order to make sure the irradiation density for each photocatalytic reaction is the same. A solution of 3 mL was drawn out at given time intervals, and the photocatalyst was separated by centrifugation in order to measure the absorption spectra of MB and calculate the MB concentration by using a UV-vis spectrophotometry. The photoactivity of commercial CuS and TiO_2 powders was also investigated for a comparison under the same conditions. The photodegradation (%) of MB was calculated by the following formula.

$$\text{Degradation (\%)} = (1 - A_t/A_0) \times 100\%$$

Where, A_0 and A_t represent the initial absorbance of MB at 664 nm and the absorbance at time t, respectively.

3. Results and Discussion

3.1. Structural and morphological characterizations

As described in the experimental section, the solvothermal synthesis of CuS structures basically involves a reaction between copper chloride and sodium thiosulfate at 150 ^oC in a mixed solvents of EG and ET. Figure 1 illustrates the FESEM images of various samples with different magnifications, which reveals that different hierarchical structures are achieved by tuning the solvent volume ratios of EG:ET. Overall the shapes of the hierarchical structures evolve from microspheres to microflowers with the increasing amount of ethanol solvent present in the synthesis reaction. The microspheres with average diameters of 2-4 μm were achieved in the absence of ET (Figure 1a-d). The higher magnified FESEM images show that these microspheres are actually composed of agglomerated nanoplates (Figure 1d). The resulting samples in the presence of small amount of ET were also sphere-like structure with smaller average microsphere diameter. For example, 2:1 EG:ET ratio leads to the formation of microspheres with diameter around 1.5 μm ((Figure 1e-f). However, flower-like structures could be achieved by increasing the EG:ET ratio from 1:1 to 1:3 (Figure 1g-l). These 3D hierarchical microflowers also exhibit self-assembled nanoplates and voids between the neighboring nanoplates. Indeed, it is revealed by TEM observation that the representative microflowers obtained with EG:ET 1:1 are composed of stacked plates, and the edge length of the plates is around 1.0 μm (Figure 3a). Kundu et al. have reported the synthesis of various CuS nanostructures by varying the solvent volume ratio of water:EG in a reaction between $Cu(NO_3)_2$ and $Na_2S_2O_3$.[41] They observed the formations of spheres consisting nanoplates in the presence of water alone, nanotubes in the case of

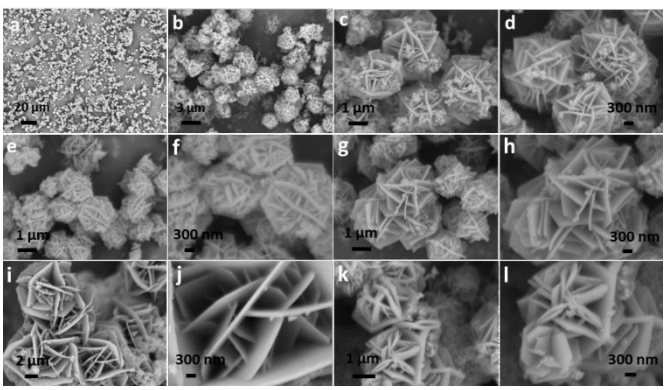

Figure 1. FESEM images in different magnifications of CuS hierarchical structures achieved with different EG:ET solvent volume ratios. (a-d) 1:0, (e-f) 2:1, (g-h) 1:1, (i-j) 1:2 and (k-l) 1:3.

1:1 water:EG solvent ratio, and sphere-like clusters in the presence of EG alone. In contrast, we obtained microspheres consisting nanoplates when EG alone was used as solvent. These results indicate that the type of precursors might play important role in controlling the morphologies of CuS.

Besides precursors of Cu and S and solvents, other synthesis parameters such as surfactants, reaction temperature, etc., have been also reported to play a critical role in the morphology-controlled nanostructures of $Cu_{2-x}S$ in a solvothermal procedure.[33, 42] Tanveer et al reported that mixed architectures of spherical and hierarchical structures of covellite CuS with inconsistency in shape and size were achieved by using ethylenediamine as solvent, however solvent diethylene glycol instead led to mainly hollow nanospheres of CuS coupled with rattle like architectures.[42] Additionally, influence of surfactant PVP was also investigated in their work, which demonstrated that hollow microspheres with a highly consistent size and shape could be obtained in the presence of higher amount of PVP, however less PVP instead resulted in irregular spherically aggregated microstructure with spherical particles attached on their surface. It was reported that increasing the amount of surfactant cetyltrimethylammonium bromide (CTAB) facilitated the formation of regular hexagonal nanoplates due to the sufficient capping to CuS by CTAB in a reaction of $CuCl_2$ with $Na_2S_2O_3$.[43]

We noticed that overall the CuS nanoplates of the microspheres obtained in the presence of EG alone are smaller in size than that of nanoplates of the microflowers achieved with mixed solvent of EG and ET. This evolution as well as the morphological evolution from microspheres to microflowers could be explained by the variation of the viscosity and stabilizing properties of the solvents present in the reaction system. EG was reported to serve as not only solvent but also stabilizing agent in the synthesis of metal (Pt, Ru) nanoparticles (NPs).[44] FTIR spectrum analysis confirmed that the stabilization by EG in CuS synthesis occurred through OH^-.[41] In the present work, Cu_xS nuclei is formed first by the reaction of Cu and S precursors, followed by the growth of plate-shaped NCs due to the intrinsic anisotropic characteristics of the CuS hexagonal crystal structure.[45] On the other side, during the formation of hexagonal CuS nanoplates, the competition between particle growth and nucleation is partially controlled by diffusion process,[46] which is dependent on the properties of solvents and surfactants. Higher solvent ratio of ET results in faster diffusion rate due to its lower viscosity (relative to EG), and thus leads to larger size of CuS nanoplates. Furthermore, higher volume ratio of ET also leads to weaker stabilization capacity and thus less self-assembly structures are expected, which allows the conversion from microspheres to microflowers by increasing ET amount.

The crystallinity of the samples was examined by XRD characterization (Figure 2a), which revealed that the diffraction patterns of all the as-synthesized structures are compatible with hexagonal structure of covellite CuS (space group: $P6_3/mmc$, JCPDS Card 06-0464). No additional diffraction peaks from other phase or impurities could be observed, suggesting the high purity of the resulting covellite CuS structures. On the other side, HRTEM image of single plate revealed a lattice spacing of around 1.9 Å, which could be indexed to (110) plane of the hexagonal covellite (CuS) phase (Figure 3b). Furthermore, energy dispersive X-ray spectra (EDS) reveals that the Cu to S atomic ratio of the as-synthesized sample is around 1:1. All these results confirm the formation of covellite CuS crystal structure.

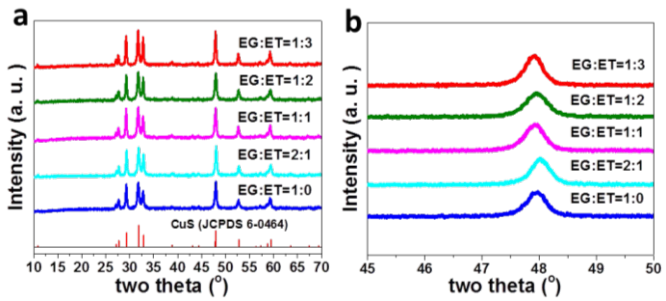

Figure 2. (a) XRD patterns of various CuS hierarchical structures achieved with different solvent volume ratios of EG:ET. (b) XRD patterns of CuS samples displaying (110) diffraction planes.

According to the full width at half-maximum (fwhm) of the diffraction peak, the average crystallite size of the CuS can be estimated from the Scherrer equation (eq. 1) and reported in Table S1 (see the supporting information).

$$D_{hkl} = K\lambda/(\beta_{hkl}\cos\theta_{hkl}) \quad (1)$$

Where D_{hkl} is the particle size perpendicular to the normal line of (hkl) plane, K is a constant (0.9), β_{hkl} is the full width at half-maximum of the (hkl) diffraction peak, θ_{hkl} is the Bragg angle of (hkl) peak, and λ is the wavelength of X-ray.

Similar with the previously reported synthesis of CuS structures in the presence of EG, the formation of covellite CuS in our case might involves the dehydration of solvent EG which leads to formation of aldehyde and water (eqn (2)),[41,47,48] and subsequent reaction between Cu^+ and S^{2-} (eqn (3)).

$$HOCH_2CH_2OH \Leftrightarrow CH_3CHO + H_2O \quad (1)$$

$$CH_3CHO + H_2O + Cu(Cl)_2 + Na_2S_2O_3 \rightarrow 2CuS\downarrow + CH_3COOH + 2NaCl + 2HCl \quad (2)$$

It is noteworthy that the present solvothermal procedure involves the mixing precursors of Cu and S in solvents and heating up to the desired temperature, which in principle is suitable for large-scale synthesis.[49] This is different with other synthesis procedures such as hot-injection which invokes a fast injection of precursors and thus is unsuitable for up-scaling production.

3.2. Optical properties

Figure 4a provides the optical spectra of the representative CuS hierarchical structures achieved with different EG:ET volume ratios (1:0, 1:1, and 1:3). The broad feature in the 330-600 nm wavelength range is attributed to excitonic absorption from covellite CuS compound.[50] The optical band gaps (Eg) are determined from their

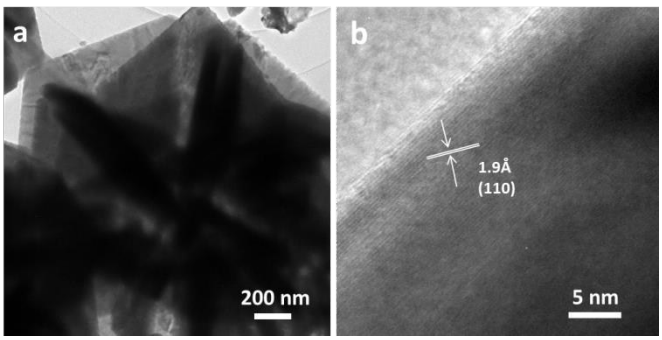

Figure 3. TEM and HRTEM images of the CuS structure obtained with 1:1 EG:ET solvent ratio. (a) TEM image; (b HRTEM image of a single hexagonal CuS nanoplate lying flat on the amorphous-carbon-coated copper grid.

optical spectra by extrapolation of the linear region of band gap plot of $(\alpha h\nu)^2$ versus energy (=hν) (see Figure S2 in the supporting information), where α is a corresponding absorption, h is plank constant, ν is frequency, and hν is the photon energy. The band gap values of the CuS structures obtained with EG:ET ratios of 1:0, 1:1 and 1:3, are respectively estimated to be 2.02, 2.02, and 2.04 eV. These results are in the range of band gap of covellite CuS reported previously,[41, 51] and also indicate that the morphology of CuS in our case have no much effect on the band gap. Besides the excitonic absorbance in the visible region, the CuS samples exhibit additional very broad absorbance in the NIR region (Figure 4a), which could be attributed to localized surface plasmon resonance of copper sulfide. Compared with the covellite nanoplates previously reported,[52] these microspheres and microflowers exhibit weaker and broader NIR plasmonic absorbance with significant red shift, which might be due to the agglomeration of the resulting plates and the big size of the hierarchical structure.

The representative covellite CuS hierarchical structures were further characterized by the PL spectroscopy in acetone at room temperature, as depicted in Figure 4b. Although it was reported that CuS does not show emission peaks in the 400-800 region,[20] both the microspheres and the microflowers in our work exhibit an intense emission peak at around 423 nm and weak peaks in the range of 475-550 nm by using a 370 nm excitation wavelength. The emission around 423 nm in CuS and $Cu_{1.8}S$ has also been reported by Kumar et al. [47] The appearance of the weak peaks in 475-550 nm region are consistent with that reported by Yang et al. and Zhu et al., which might be due to the surface defects and an interface coupling effect between the grain boundaries.[53-55] The minor shift in peak position in different samples might be due to the difference of the morphologies (shape and size) (Figure 4b), which was also discussed in the hierarchical architectures of covellite CuS.[48] This makes sense since the nature of the emission spectra of CuS depends on not only the inherent structure but also the morphology. [41, 47, 56]

3.3. Photocatalytic activities

The narrow band gaps of the resulting CuS hierarchical structures allow us the application of these materials for photocatalysis under visible or natural irradiation. Consequently, we tested the photocatalytic activities of the as-synthesized CuS samples in MB degradation under natural light irradiation in the presence of H_2O_2. Figure 5A illustrates the curves of the MB photodegradation versus the irradiation time. The characteristic absorption peak of MB at 662 nm was used to monitor the photocatalytic process and to calculate the degradation efficiency. It was noted that H_2O_2 is critical for the photocatalysis on CuS,[42, 57] although the degradation of MB could be negligible in the presence of only H_2O_2 (Figure 5aI). On the other side, we observed little change of the MB concentration under darkness after reaching the adsorption/desorption equilibrium between MB molecules and the CuS surface. All these observations confirmed that the decrease of MB concentration under natural light irradiation in the presence of CuS is indeed due to the photodegradation process. As depicted in Figure 5a and Figure S3, the degradation performance of various photocatalysts follows the order: EG:ET = 1:1 (99.2%) > 1:2 (98.6%) > 1:0 (95.6%) > 2:1 (94.7%) > 1:3 (92.7%) > commercial TiO_2 (86.3%) > commercial CuS (49.9%). That is, the CuS microflowers obtained with 1:1 EG:ET ratio display the best photocatalytic activity as compared with all the other photocatalysts discussed herein.

The photocatalytic stability of the CuS photocatalyst (EG:ET=1:1) was further investigated by repeating the MB degradation for five cycles, under the same degradation conditions in each cycle. In each recycle, the CuS photocatalyst was separated by centrifugation and washed with ethanol before re-using for photodegradation. Figure 5b presents the plot of degradation percentage as a function of cycle number, which indicates that the photocatalytic efficiency of CuS decreased only 3.1 % after five cycles. It is noteworthy that no change of crystal structure could be observed on the CuS even after 5 cycles of photocatalysis, which is confirmed by XRD characterization (Figure S4). These results suggest that the CuS exhibits good stability and robustness as photocatalyst.

It has been generally accepted that the photocatalytic efficiency is predominantly correlated with the separation/recombination of photo-excited electron/hole pairs, the morphologies, specific surface area, crystallinity, particle size, the adsorption/desorption of organic molecules on the catalyst surface, etc. [48,58] In order to figure out the surface area and the porosity, the representative samples are investigated by N_2 adsorption/desorption isotherms. It reveals a characteristic type IV isotherm in Figure S5a. The calculation results of surface area and pore size based on BET and BJH methods, respectively, are provided in Table S1, which indicate a wide pore size distribution. Compared with other photocatalysts, the priority of photocatalytic activity the CuS microflowers obtained with 1:1 EG:ET ratio could be attributed to the following parameters: a) The presence of surface defects on the CuS nanoplates, which are indicated by PL analysis, can act as electron acceptors and thus facilitate the efficient separation of photo-excited electron/hole pairs.[54] b) The CuS obtained with EG:ET 1:1 has smaller surface area compared with other CuS samples (Table S1), however it shows larger average pore size. The presence of large pores favors enhanced diffusion of the dye molecules and thus facilitates the photodegradation.[58] c) The CuS nanoplates of this unique flower-like hierarchical structure can serve as "mirrors" and the photoabsorption can be enhanced by the reflection among the nanoplates.[57] d) Compared with TiO_2, the CuS photocatalyst can effectively utilize visible energy from the natural light.

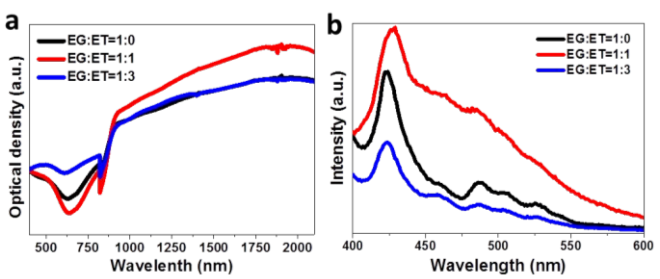

Figure 4. (a) UV-vis-NIR spectra, and (b) room temperature photoluminescence of the CuS hierarchical structures achieved in the presence of 1:0, 1:1 and 1:3 EG:ET solvent volume ratios, respectively.

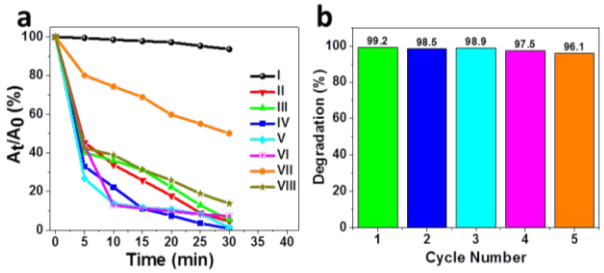

Figure 5. (a) Photodegradation efficiencies of MB as a function of natural light irradiation time by various photocatalysts. (I) in the presence of only H_2O_2, (II) EG:ET=1:0, (III) EG:ET=2:1, (IV) EG:ET=1:1, (V) EG:ET=1:2, (VI) EG:ET=1:3, (VII) commercial CuS and (VIII) commercial TiO_2. (b) Photocatalysis stability test of the as-synthesized CuS for MB degradation.

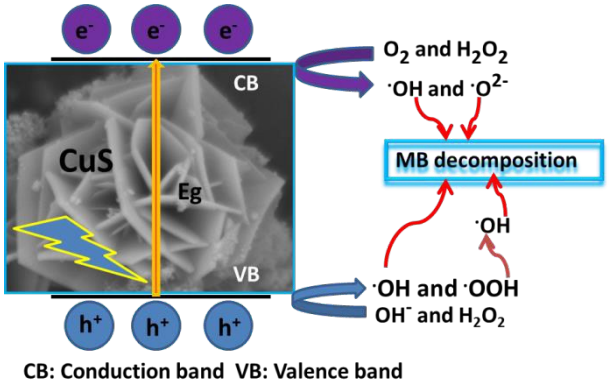

Figure 6. Mechanism of the MB photodegradation on CuS photocatalyst.

Although CuS with 1:1 EG:ET exhibits the highest photocatalytic efficiency among the various samples discussed herein, we noted that other CuS hierarchical structures also exhibit close photocatalytic activity for the MB photodegradation (Figure S4). This good photocatalytic activity of CuS hierarchical structures has been investigated by evaluating the decomposition rate of cationic dye MB solution in the presence of H_2O_2 under natural light.[11] The photodegradation of other dye molecules (cationic dyes like rhodamine B (RhB), malachite green (MG), neutral dye like methyl red (MR), and anionic dyes like methyl orange (MO) and eosin) were also researched on hierarchical hexagonal stacked plates of CuS under indoor illumination.[10] In this work, the degradation kinetics is observed to be quite faster for the cationic dye molecules than neutral and anionic ones. This is because CuS photocatalyst inherits negative surface charge due to the surface bound OH^- ions, which facilitates the attraction of cationic dye molecules to the catalyst surface and subsequently facilitates the electron transfer [54] to enhance the photodegradation efficiency.

Overall the mechanism of converting solar energy to chemical energy in photocatalysis of $Cu_{2-x}S$ is similar with that of extensively researched TiO_2 photocatalyst, except that electrons (e^-) and holes (h^+) could be excited even under visible irradiation, to the conduction band and the valence band edge, respectively (Figure 6) (eqn (3)).[12, 42, 57] These photo-excited e^- and h^+ then can transfer to the surface of the photocatalyst (CuS particles), where they react with oxidants and reductants, respectively, or recombine in the absence of e^- and h^+ traps. For example, the excited e^- reacts with dissolved O_2 to form $\cdot O_2^-$ (eqn (5)), while h^+ reacts with surface hydroxyl groups to form hydroxyl radicals ($\cdot OH$) (eqn (6)).[10, 59] The recombination of e^- - h^+ could be greatly minimized in the presence of H_2O_2, which traps the e^- and h^+ to form $\cdot OH$ and $\cdot O_2^-$ species (eqn (7)-(9)).[42, 60] It was reported that the accumulated e^- in the CB can be also transferred to oxygen to form H_2O_2,[12] which could be further reduced to $\cdot OH$. Organic contamination molecules such as MB, could be decomposed to intermediates or mineralized products through an oxidation reaction by the so-formed $\cdot OH$ or $\cdot O_2^-$ species (Figure 6) (eqn. (10)),[61] or directly by the holes accumulated in the VB.[62, 63]

$$CuS + h\nu \rightarrow h^+(CuS) + e^-(CuS) \quad (3)$$
$$H_2O \rightarrow H^+ + OH^- \quad (4)$$
$$e^-(CuS) + O_2 \rightarrow \cdot O_2^- \quad (5)$$
$$h^+(CuS) + OH^- \rightarrow \cdot OH \quad (6)$$
$$e^-(CuS) + H_2O_2 \rightarrow \cdot OH + OH^- \quad (7)$$
$$h^+(CuS) + H_2O_2 \rightarrow \cdot OOH + H^+ \quad (8)$$
$$\cdot OOH \rightarrow \cdot O_2^- + H^+ \quad (9)$$
$$MB + \cdot OH + \cdot O_2^- \rightarrow \text{degradation products} \quad (10)$$

3.4. Hierarchical structure of CuS obtained with DMF solvent

For comparison, we also prepared covellite CuS structures by using DMF instead of EG/ET as solvent, and the structural, optical and morphological characterization and photocatalysis are depicted in Figure 7. Irregular sphere-like hierarchical structure consisting nanoplates was generated, which is similar with the hierarchical architectures of CuS obtained by reacting $Cu(NO_3)_2 \cdot 3H_2O$ with thiourea in a DMF solvent.[42] The decomposition of MB on this sample is 63.0 % under the same conditions of photocatalysis discussed above, indicates that it's photocatalytic activity is lower than other CuS hierarchical structures obtained in EG/ET solvents but higher than commercial CuS photocatalyst.

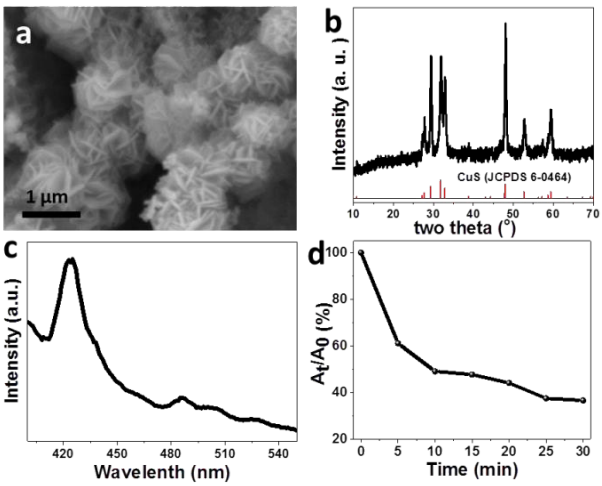

Figure 7. The results of CuS achieved by using DMF as solvent: (a) SEM image, (b) XRD pattern, (c) optical spectra (inset is PL), and (d) photodegradation efficiencies of MB.

4. Conclusions

In summary, we have demonstrated a simple and effective solvothermal procedure for synthesis of hierarchical structures of covellite CuS nanoplates. It is revealed that the morphology and size could be tuned by choosing different solvents of EG, ET and DMF, and by tailoring the EG:ET volume ratio. The solvent DMF alone leads to the formation of irregular sphere-like hierarchical structure. Microspheres consisting CuS nanoplates are also achieved in the presence of solvent EG alone, or in a mixed solvent with EG:ET over 1:1. However microflowers composed of CuS plates are formed in the presence of more ET (1:1 to 1:3 of EG:ET). The band gap energies of the resulting hierarchical structures are estimated to be around 2.02-2.04 eV. Furthermore, the photocatalytic efficiency of the as-synthesized CuS hierarchical structures for MB degradation under natural irradiation is higher than that of commercial TiO_2 and almost two times of commercial CuS powders. The hierarchical CuS microflowers achieved with 1:1 EG:ET exhibits the priority of activity over other photocatalysts and demonstrates excellent photocatalytic stability and recycling capability, without significant loss of efficiency and change of crystal phase upon 5 cycles of photocatalysis. In principle, the solvothermal approach present here could be suitable for up-scaling synthesis of CuS, and might be exploited to the synthesis of other semiconducting micro- and

nanostructures for potential applications in the fields of optics, sensors, environmental pollution, and so forth.

Acknowledgements

The authors would like to thank the University of Tabriz and Iranian Nanotechnology Initiative Council for the financial support of this project. Authors also acknowledge Istituto Italiano di Tecnologia (IIT) for the UV-Vis-NIR and PL characterizations, and State Key Laboratory of Silicate Materials for Architectures (Wuhan University of Technology) for TEM/HRTEM measurement.

* Corresponding authors.

Notes and references

[a] *Department of Inorganic Chemistry, Faculty of Chemistry, University of Tabriz, bolvar 29 bahman, Tabriz, Iran.Tel: +98-413-3393130, Fax: +98-413-3340191, E-mail: Z.Hosseinpour@tabrizu.ac.ir (Zahra Hosseinpour).*
[b] *Department of Nanochemistry, Istituto Italiano di Tecnologia (IIT), via Morego, 30, 16163 Genova, Italy. Tel: +39-3778367185, E-mail: Yi.Xie@iit.it, xieyithanks@163.com (Yi Xie).*
[c] *State Key Laboratory of Silicate Materials for Architectures, Wuhan University of Technology, Wuhan 430070, Hubei Province, People's Republic of China*

References

1. A. Fujishima and K. Honda, *Nature*, 1972, **238**, 37-38.
2. M. Ni, M. K. H. Leung, D. Y. C. Leung and K. Sumathy, *Renewable and Sustainable Energy Reviews*, 2007, **11**, 401-425.
3. A. L. Linsebigler, G. Lu and J. T. Yates, *Chemical Reviews*, 1995, **95**, 735-758.
4. K. Sunada, Y. Kikuchi, K. Hashimoto and A. Fujishima, *Environmental Science & Technology*, 1998, **32**, 726-728.
5. Y. Xie, X. Zhao, Y. Chen, Q. Zhao and Q. Yuan, *Journal of Solid State Chemistry*, 2007, **180**, 3576-3582.
6. R. Asahi, T. Morikawa, H. Irie and T. Ohwaki, *Chemical Reviews*, 2014, **114**, 9824-9852.
7. J. Schneider, M. Matsuoka, M. Takeuchi, J. Zhang, Y. Horiuchi, M. Anpo and D. W. Bahnemann, *Chemical Reviews*, 2014, **114**, 9919-9986.
8. Y. Xie and X. Zhao, *Journal of Molecular Catalysis A: Chemical*, 2008, **285**, 142-149.
9. J. C. Yu, Yu, Ho, Jiang and Zhang, *Chemistry of Materials*, 2002, **14**, 3808-3816.
10. M. Basu, A. K. Sinha, M. Pradhan, S. Sarkar, Y. Negishi, Govind and T. Pal, *Environmental Science & Technology*, 2010, **44**, 6313-6318.
11. F. Li, J. Wu, Q. Qin, Z. Li and X. Huang, *Powder Technology*, 2010, **198**, 267-274.
12. M. Peng, L.-L. Ma, Y.-G. Zhang, M. Tan, J.-B. Wang and Y. Yu, *Materials Research Bulletin*, 2009, **44**, 1834-1841.
13. M. Shalom, M. Guttentag, C. Fettkenhauer, S. Inal, D. Neher, A. Llobet and M. Antonietti, *Chemistry of Materials*, 2014, **26**, 5812-5818.
14. P. Wang, B. Huang, X. Qin, X. Zhang, Y. Dai, J. Wei and M.-H. Whangbo, *Angewandte Chemie International Edition*, 2008, **47**, 7931-7933.
15. Y. Yang, G. Zhang, S. Yu and X. Shen, *Chemical Engineering Journal*, 2010, **162**, 171-177.
16. L. Zhang, W. Wang, Z. Chen, L. Zhou, H. Xu and W. Zhu, *Journal of Materials Chemistry*, 2007, **17**, 2526-2532.
17. M. Tanveer, C. Cao, I. Aslam, Z. Ali, F. Idrees, W. S. Khan, M. Tahir, S. Khalid, G. Nabi and A. Mahmood, *New Journal of Chemistry*, 2015, **39**, 1459-1468.
18. C. Ratanatawanate, A. Bui, K. Vu and K. J. Balkus, *The Journal of Physical Chemistry C*, 2011, **115**, 6175-6180.
19. R. Blachnik and A. Müller, *Thermochimica Acta*, 2000, **361**, 31-52.
20. X. Jiang, Y. Xie, J. Lu, W. He, L. Zhu and Y. Qian, *Journal of Materials Chemistry*, 2000, **10**, 2193-2196.
21. L. Chen, W. Yu and Y. Li, *Powder Technology*, 2009, **191**, 52-54.
22. T. Sakamoto, H. Sunamura, H. Kawaura, T. Hasegawa, T. Nakayama and M. Aono, *Applied Physics Letters*, 2003, **82**, 3032-3034.
23. J. S. Chung and H. J. Sohn, *Journal of Power Sources*, 2002, **108**, 226-231.
24. A. Šetkus, A. Galdikas, A. Mironas, I. Šimkiene, I. Ancutiene, V. Janickis, S. Kaciulis, G. Mattogno and G. M. Ingo, *Thin Solid Films*, 2001, **391**, 275-281.
25. X.-P. Shen, H. Zhao, H.-Q. Shu, H. Zhou and A.-H. Yuan, *Journal of Physics and Chemistry of Solids*, 2009, **70**, 422-427.
26. Z. R. Dai, Z. W. Pan and Z. L. Wang, *Journal of the American Chemical Society*, 2002, **124**, 8673-8680.
27. K. A. Dick, K. Deppert, M. W. Larsson, T. Martensson, W. Seifert, L. R. Wallenberg and L. Samuelson, *Nat Mater*, 2004, **3**, 380-384.
28. D. Wang and C. M. Lieber, *Nat Mater*, 2003, **2**, 355-356.
29. H. Zhang, Y. Zhang, J. Yu and D. Yang, *The Journal of Physical Chemistry C*, 2008, **112**, 13390-13394.
30. Y. Xie, A. Riedinger, M. Prato, A. Casu, A. Genovese, P. Guardia, S. Sottini, C. Sangregorio, K. Miszta, S. Ghosh, T. Pellegrino and L. Manna, *Journal of the American Chemical Society*, 2013, **135**, 17630-17637.
31. H. T. Zhang, G. Wu and X. H. Chen, *Materials Chemistry and Physics*, 2006, **98**, 298-303.
32. P. Roy and S. K. Srivastava, *Crystal Growth & Design*, 2006, **6**, 1921-1926.
33. Z. Cheng, S. Wang, Q. Wang and B. Geng, *CrystEngComm*, 2010, **12**, 144-149.
34. W. Du, X. Qian, X. Ma, Q. Gong, H. Cao and J. Yin, *Chemistry – A European Journal*, 2007, **13**, 3241-3247.
35. M. Nagarathinam, K. Saravanan, W. L. Leong, P. Balaya and J. J. Vittal, *Crystal Growth & Design*, 2009, **9**, 4461-4470.
36. Y. Du, Z. Yin, J. Zhu, X. Huang, X.-J. Wu, Z. Zeng, Q. Yan and H. Zhang, *Nat. Commun.*, 2012, **3**, 1-7.
37. e. a. H. Katagiri, Appl. Phys. Express 2008, vol. 1, 041201.
38. S. He, G.-S. Wang, C. Lu, X. Luo, B. Wen, L. Guo and M.-S. Cao, *ChemPlusChem*, 2013, **78**, 250-258.
39. L. Mi, W. Wei, Z. Zheng, Y. Gao, Y. Liu, W. Chen and X. Guan, *Nanoscale*, 2013, **5**, 6589-6598.
40. S.-J. Liu, Y.-F. Hou, S.-L. Zheng, Y. Zhang and Y. Wang, *CrystEngComm*, 2013, **15**, 4124-4130.
41. J. Kundu and D. Pradhan, *ACS Applied Materials & Interfaces*, 2014, **6**, 1823-1834.
42. M. Tanveer, C. Cao, Z. Ali, I. Aslam, F. Idrees, W. S. Khan, F. K. But, M. Tahir and N. Mahmood, *CrystEngComm*, 2014, **16**, 5290-5300.
43. L. Chu, B. Zhou, H. Mu, Y. Sun and P. Xu, *Journal of Crystal Growth*, 2008, **310**, 5437-5440.
44. J. Yang, T. C. Deivaraj, H.-P. Too and J. Y. Lee, *Langmuir*, 2004, **20**, 4241-4245.
45. M. Saranya, C. Santhosh, R. Ramachandran and A. Nirmala Grace, *Journal of Nanotechnology*, 2014, **2014**, 8.
46. B. Li, Y. Xie, J. Huang, Y. Liu and Y. Qian, *Chemistry of Materials*, 2000, **12**, 2614-2616.
47. P. Kumar, M. Gusain and R. Nagarajan, *Inorganic Chemistry*, 2011, **50**, 3065-3070.
48. M. Tanveer, C. Cao, I. Aslam, Z. Ali, F. Idrees, M. Tahir, W. S. Khan, F. K. Butt and A. Mahmood, *RSC Advances*, 2014, **4**, 63447-63456.
49. E. Dilena, Y. Xie, R. Brescia, M. Prato, L. Maserati, R. Krahne, A. Paolella, G. Bertoni, M. Povia, I. Moreels and L. Manna, *Chemistry of Materials*, 2013, **25**, 3180-3187.

50. Y. Zhao, H. Pan, Y. Lou, X. Qiu, J. Zhu and C. Burda, *Journal of the American Chemical Society*, 2009, **131**, 4253-4261.
51. J. Santos Cruz, S. Mayén Hernández, F. Paraguay Delgado, O. Zelaya Angel, R. Castanedo Pérez and G. Torres Delgado, *International Journal of Photoenergy*, 2013, **2013**.
52. Y. Xie, L. Carbone, C. Nobile, V. Grillo, S. D'Agostino, F. Della Sala, C. Giannini, D. Altamura, C. Oelsner, C. Kryschi and P. D. Cozzoli, *ACS Nano*, 2013, **7**, 7352-7369.
53. E. Ramli, T. B. Rauchfuss and C. L. Stern, *Journal of the American Chemical Society*, 1990, **112**, 4043-4044.
54. Z. K. Yang, L. X. Song, Y. Teng and J. Xia, *Journal of Materials Chemistry A*, 2014, **2**, 20004-20009.
55. H. Zhu, J. Wang and D. Wu, *Inorganic Chemistry*, 2009, **48**, 7099-7104.
56. K. P. Kalyanikutty, M. Nikhila, U. Maitra and C. N. R. Rao, *Chemical Physics Letters*, 2006, **432**, 190-194.
57. Y.-Q. Zhang, B.-P. Zhang, Z.-H. Ge, L.-F. Zhu and Y. Li, *European Journal of Inorganic Chemistry*, 2014, **2014**, 2368-2375.
58. S. Rasalingam, C.-M. Wu and R. T. Koodali, *ACS Applied Materials & Interfaces*, 2015, **7**, 4368-4380.
59. S. Kuriakose, B. Satpati and S. Mohapatra, *Phys. Chem. Chem. Phys.*,, 2014, **16**, 12741-12749.
60. S. Sun, X. Song, D. Deng, X. Zhang and Z. Yang, *Catalysis Science & Technology*, 2012, **2**, 1309-1314.
61. Z. K. Yang, L. X. Song, Y. Teng and J. Xia, *Journal of Materials Chemistry A*, 2014.
62. J. Sun, X. Yan, K. Lv, S. Sun, K. Deng and D. Du, *Journal of Molecular Catalysis A: Chemical*, 2013, **367**, 31-37.
63. Y. Xie, G. Ali, S. H. Yoo and S. O. Cho, *ACS Applied Materials & Interfaces*, 2010, **2**, 2910-2914.